J. Membrane Biol. 96, 27–43 (1987)

The Journal of
Membrane Biology


# Cell Membrane Water Permeability of Rabbit Cortical Collecting Duct

Kevin Strange* and Kenneth R. Spring
Laboratory of Kidney and Electrolyte Metabolism, National Heart, Lung, and Blood Institute, National Institutes of Health, Bethesda, Maryland 20892

**Summary.** The water permeability ($P_{osm}$) of the cell membranes of isolated perfused rabbit cortical collecting ducts was measured by quantitative light microscopy. Water permeability of the basolateral membrane, corrected for surface area, was 66 $\mu m \cdot sec^{-1}$ for principal cells and 62.3 $\mu m \cdot sec^{-1}$ for intercalated cells. Apical membrane $P_{osm}$ values corrected for surface area, were 19.2 and 25 $\mu m \cdot sec^{-1}$ for principal and intercalated cells, respectively, in the absence of antidiuretic hormone (ADH). Principal and intercalated cells both responded to ADH by increasing $P_{osm}$ of their apical membranes to 92.2 and 86.2 $\mu m \cdot sec^{-1}$, respectively. The ratio of the total basolateral cell membrane osmotic water permeability to that of the apical cell membrane was ~27 : 1 in the absence of ADH and ~7 : 1 in the presence of the hormone for both cell types. This asymmetry in water permeability is most likely due to the fact that basolateral membrane surface area is at least 7 to 8 times greater than that of the apical membrane. Both cell types exhibited volume regulatory decrease when exposed to dilute serosal bathing solutions. Upon exposure to a hyperosmotic serosal bath (390 mosM), principal cells did not volume regulate while two physiologically distinct groups of intercalated cells were observed. One group of intercalated cells failed to volume regulate; the second group showed almost complete volume regulatory increase behavior.

**Key Words** light microscopy · antidiuretic hormone · epithelial cell volume · principal cell · intercalated cell · volume regulation

## Introduction

Measurements of cell membrane water permeability ($P_{osm}$) are crucial for understanding the routes and driving forces for fluid movement across epithelia and the osmotic relations of epithelial cells. To date, $P_{osm}$ has been measured directly in the apical and basolateral membranes of *Necturus* gallbladder [28] and rabbit proximal straight tubule [6, 14, 41], basolateral membranes of rabbit proximal convoluted tubule [41] and apical membrane of toad bladder granular cells [21].

The cortical collecting duct is one of the major sites of action of antidiuretic hormone (ADH). In the presence of the hormone, the transepithelial water permeability and water reabsorption of this nephron segment are increased dramatically (reviewed in ref. 18). Cortical collecting ducts of the rabbit are composed of principal and intercalated cells present in a ratio of *ca.* 2 : 1 [22]. No direct, and very little indirect evidence exists, but it is generally believed that the principal cell apical membrane is the site of ADH action (e.g., ref. 22). Recently, studies in toad bladder have suggested that ADH may also alter the water permeability of a barrier distal to the apical membrane [21].

In the present study we measured $P_{osm}$ of the apical and basolateral membranes of both principal and intercalated cells. We also tested the effects of ADH on $P_{osm}$ of both membranes in each cell type. In addition, we examined the ability of cortical collecting duct cells to volume regulate after exposure to hyperosmotic or hypoosmotic perfusates. These investigations were undertaken both to establish a general approach for measurement of $P_{osm}$ in cells of isolated nephron segments and to provide a more detailed understanding of the control of water movement across principal and intercalated cell membranes.

## Materials and Methods

### Tubule Perfusion

NIH New Zealand white female rabbits (1.0 to 1.5 kg) were maintained on Purina rabbit chow and tap water *ad libitum*. Rabbits were sacrificed by decapitation and both kidneys removed immediately and transferred to ice-cold control saline (*see below*). Segments of cortical collecting ducts were dissected from kidney slices in a bath chamber maintained at 15°C and gassed with 95% $O_2$–5% $CO_2$. Care was taken to isolate only segments lacking adherent thick ascending limbs and large amounts of interstitial tissue.

* *Present address:* Department of Physiology and Biophysics, Wright State University School of Medicine, Dayton, OH 45435.

Tubule perfusion methods were similar to those described in detail previously [35]. Briefly, the tubule was transferred to a laminar flow bath chamber and one end was drawn up into a conventional glass-holding pipette. The tubule was cannulated and perfused using an inner concentric perfusion pipette. The distal end of the tubule was held in place with another glass-holding pipette. Exposed tubule lengths of 400 to 500 $\mu$m were used to minimize tubule movements. Once the tubule was in place, bath perfusion was initiated and maintained at 4–6 ml · $min^{-1}$ for at least a 1-hr equilibration period. Just prior to switching serosal solution composition the bath flow rate was increased to 10 ml · $min^{-1}$.

We did not measure luminal perfusion rate directly in these studies and instead relied on using high perfusion pressures (40 to 50 cm $H_2O$) to maintain a high luminal solution flow to prevent changes in perfusate concentration. Observation of particle movement through the lumen indicated a perfusion rate significantly $> 30$ nl · $min^{-1}$. Cell volume measurements were made at varying distances from the perfusion pipette tip. The osmometric response of intercalated and principal cells exposed to mucosal hypertonicity (Table 5) in the presence of a serosal oil bath and the small variability in apical $P_{osm}$ measurements indicate that there was no dissipation of the luminal osmolality gradient due to transepithelial water movement.

## Bath Chamber Design

Tubules were suspended in bath chamber designed for rapid fluid exchange and to minimize movement of the preparation. As previously described [35], bath exchange time was measured by focusing a 50-$\mu$m spot of light between a set of holding pipettes and monitoring the wash in of dye using a computer-interfaced photomultiplier tube. Half-times for complete bath exchange at a flow rate of 10 ml · $min^{-1}$ were between 55 and 60 msec. Serosal unstirred layers were less than 3 $\mu$m in thickness as determined from the flow patterns of latex beads around the tubule [35]. Bath temperature and pH were closely regulated at 37°C and 7.4, respectively [35].

## Microscopy

The bath chamber was mounted on the stage of an inverted microscope (Nikon, Diaphot; Nikon Microscope Inc., Garden City, N.Y.) modified for tubule perfusion. The perfusion apparatus was attached to micromanipulators mounted directly to the microscope stage. Linear translation stages (Model MR 80; Klinger Scientific, Richmond Hill, N.Y.) were used to move the perfusion apparatus in the $x$- and $y$-axes. These micromanipulators were used because they provided high precision, superior stability and a low profile. A microscope focus mount (Model 740-F-PL; Rolyn Optics, Covina, Calif.) was used for the $z$-axis to provide a long translation distance with both coarse and fine adjustments. The microscope stage was modified to increase stability and provide for greater ease in translation. This arrangement of micromanipulators allowed the entire length and width of the tubule to be scanned simply by translating the microscope stage.

The microscope was equipped with differential interference contrast (DIC) optics consisting of a Glan-Thompson calcite polarizing prism (GT-NS-10 mm; Zeta International Corp., Mt. Prospect, Ill.), a mica $\frac{1}{4}$ wave plate (Esco Products Inc., Oak Ridge, N.Y.), matched Wollaston prisms (Carl Zeiss Inc., New York, N.Y.) and a Glan-Taylor calcite prism (TY-NS-12 mm; Zeta International Corp.) used as an analyzer. Tubules were viewed using a Leitz planapochromat 100× (1.32 N.A.) oil-immersion objective lens with a 250-$\mu$m working distance and a Leitz 32× (0.40 N.A.) objective-condenser lens with a 6.6-mm working distance. The 32× condenser lens was mounted on a rotating turret so it could be moved out of the way during initial tubule set up.

Tubule images were recorded using a television camera (Model NC-65S; Dage-MTI Inc., Michigan City, Ind.) and a video disc recorder (Model VDR-1RA; Precision Echo, Mountain View, Calif.) interfaced to a computer (MacSym 150; Analog Devices, Norwood, Mass.). Additional image magnification of 2.3× was provided by moving the camera away from a 1× projection lens, and by using the camera's electronic magnification option (Insta-View Option). High frequency detail in the video images was enhanced using a Model IV-530 contour synthesizer (FOR-A Corporation of America, West Newton, Mass.).

## Luminal Perfusate Exchange

The method which has been used previously for rapid exchange of solutions perfusing the tubule lumen is the double-barreled pipette method of Greger and Schlatter [15]. This approach was not acceptable for our experiments because it required several trial switches of the luminal perfusate to balance the flows in the two pipette barrels. Exposure of the tubules to test solutions prior to the recording period could possibly cause changes in intracellular factors (e.g., $Ca^{2+}$, pH) thought to control water channel insertion and retrieval [17]. In addition, previous studies have demonstrated that *Necturus* gallbladder cells show a diminished response to successive mucosal hypoosmotic perturbations [26]. We therefore devised a new system to switch the luminal solution rapidly. As described previously [35], luminal exchange was accomplished by utilization of two concentric pipettes formed to fit tightly together. Retraction of the inner pipette by means of a hydraulic arrangement enabled rapid switches of the luminal perfusate. Pipette exchange times were measured by focusing a 50-$\mu$m spot of light a short distance behind the tip of the perfusion pipette and monitoring the appearance of dye in the pipette. We tested a variety of pipette combinations at a range of perfusion pressures and found that the half-times for solution changes were 70 to 150 msec. In some experiments where we were not concerned with the rapidity of the luminal perfusate change, we used the conventional fluid exchange pipette arrangement described by Burg [5]. Luminal perfusate could be changed in *ca.* 30 sec using this pipette arrangement.

It should be noted here that the retractable pipette method did not cause changes in perfusion pressure during solution switches. The limiting resistance of the pipette arrangement is the tip of the perfusion pipette which cannulates the tubule lumen. This resistance is not altered during retraction of the inner pipette.

## Solution Composition

Tubules were bathed and perfused with a solution containing (in mM): 118 NaCl, 23 $NaHCO_3$, 2.5 $K_2HPO_4$, 1.2 $MgSO_4$, 2.0 Ca lactate$_2$, 5.5 glucose, 1.0 $Na_3$ citrate and 6.0 L-alanine. Solution osmolality was increased by the addition of raffinose. In experiments where membrane $P_{osm}$ was determined for a 100-mosM

hypoosmotic gradient, 50 mM NaCl was replaced by 100 mM raffinose in control solutions. Tubules were equilibrated in this control solution for at least 1 hr before being exposed to a hypoosmotic solution from which the raffinose was removed.

### Determination of Basolateral $P_{osm}$

We used two regions of the tubule for these studies: en face images for determination of cell volume and lateral wall images for determination of rates of cell volume change. Just prior to switching basolateral solution composition, a series of "optical sections" were recorded of a principal or intercalated cell located on the bottom of the tubule (en face view). Great care was taken to insure that the cell outline was flat and not contributing to the curvature of the tubule wall. Optical sectioning began at the basal end of the cell and video images were recorded at 1.2-$\mu$m intervals focusing towards the apical cell pole. The area and perimeter of each section were traced at a later time using a computer to digitize the cell boundaries. Cell volume was calculated as described by Spring and Hope [34]. Microscope focusing was controlled by a computer-interfaced stepping motor drive attached to the fine focus drive.

The time required to record a complete set of optical sections of a collecting duct cell (i.e., 8 to 10 sections) was 1.5 to 2.0 sec, much too slow to obtain information on rates of cell volume change. To acquire such information, we imaged cross-sections of principal and intercalated cells in the lateral tubule wall (lateral wall image). Given the high total magnification at which images were recorded, it was possible to collect data from at most two cells in any experiment. When two cells were imaged they always consisted of a single principal cell and a smaller intercalated cell (e.g., *see* Fig. 6). Once the proper focal plane had been chosen basolateral solution composition was switched; video images were then recorded at a rate of 15 frames · $sec^{-1}$. The cross-sectional area of the cell on each video frame was traced at a later time for determination of the rate of cell volume change.

### Determination of Apical $P_{osm}$

Apical $P_{osm}$ measurements were greatly complicated by the relatively high water permeability of the basolateral cell membrane. To circumvent this problem we developed the methodology to perfuse collecting ducts under oil. Prior to each experiment the bath chamber was thoroughly cleaned with ether and a dilute solution of Tween-20 and then silanized with a water-based silanizing agent (Prosil 28; PCR Research Chemicals Inc., Gainesville, Fla.). The tip of the collection-holding pipette was also thoroughly cleaned and silanized. Silanization was critical for proper adherence of the oil droplet to the bath chamber floor.

Tubules were set up and perfused as described above. Shortly before switching luminal solution composition bath flow was stopped briefly, and a small droplet of Dow-Corning 200 silicone oil (1 or 100 cs viscosity) was lodged onto the bottom of the bath chamber. The tubule was manipulated into the oil droplet and bath flow restarted at 4 to 6 ml · $min^{-1}$ to maintain temperature and gas composition. The tubule imaging protocol described above was followed and luminal solution composition was switched within 10 min after isolating the collecting duct in the oil droplet. Video images were recorded at a rate of 1 frame · $sec^{-1}$ for apical solution changes without ADH or 3 frames · $sec^{-1}$ for apical solution changes in the presence of ADH.

Apical $P_{osm}$ was measured in both the absence and presence of Arginine Vasopressin (Sigma, Grade VIII). Because of the possibility of hormone binding to the large surface areas of our glass perfusion lines and reservoirs, we used supramaximal doses of ADH (250 to 1000 $\mu$U · $ml^{-1}$) throughout these studies. All concentrations used gave the same results. Collecting ducts were initially equilibrated for at least 30 min in control solutions before being exposed to the ADH-containing solutions for an additional 30 min.

### Statistical Analysis

Data are expressed as the mean ± standard error of the mean ($n$ = number of tubules). Statistical analyses were performed using a standard Student's $t$-test.

## Results

### Cell Morphology

Microscope resolution was sufficient to distinguish clearly cell borders from basal to apical poles of cortical collecting duct cells (Figs. 1 and 2) and to observe a wide variety of directed intracellular organelle movements. In addition, we were able to easily differentiate both principal and intercalated cell types. En face principal cell images were characterized as having relatively low contrast, a hexagonal cell outline and the presence of a single cilium located on the apical cell membrane (Fig. 1).

Recent physiological studies in rabbit [30, 31, 39] and ultrastructural studies in rat [38] and rabbit [25] have suggested the presence of two distinct types of intercalated cells in cortical collecting ducts. We have also identified what appear to be two morphologically distinct populations of this cell type. One type has a circular cell outline which extends from the basal to apical pole of the cell. In any given preparation these cells are taller than adjacent principal cells causing them to bulge prominently into the tubule lumen (Fig. 2). The second intercalated cell type (*see* ref. 35) has a hexagonally shaped basal membrane similar to that of the principal cell. Towards its apical pole, this cell type tapers and shows a characteristic circular cell outline. These cells have an apical surface area similar to the first intercalated cell type and also bulge out into the tubule lumen.

Both intercalated cell types also differed from principal cells in that they had a much higher relative contrast and contained numerous large intracellular structures (*see* Fig. 2) which were possibly mitochondria. Lateral wall images of principal cells showed a distinctly rectangular shape while intercalated cells again had a circular outline (Fig. 3). We

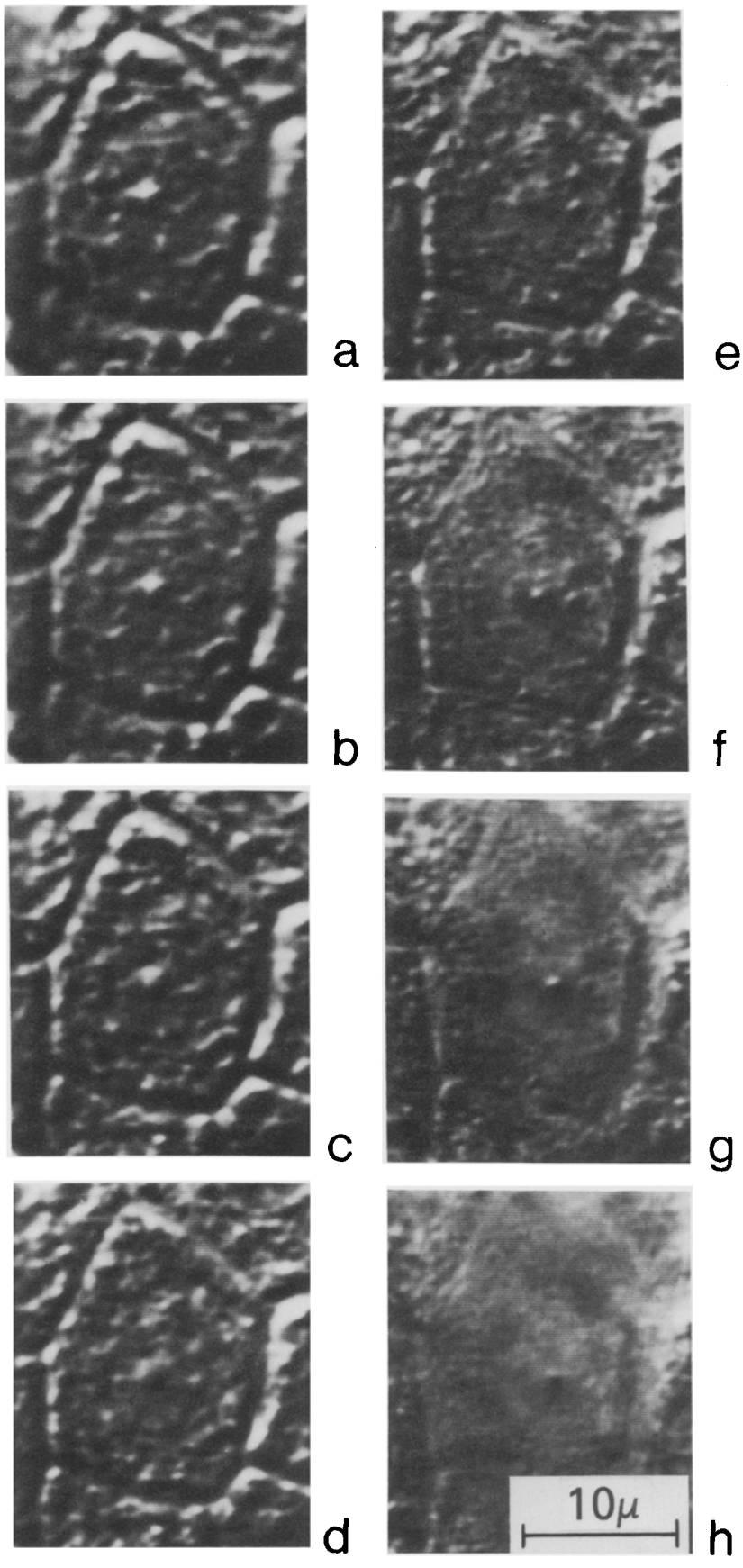


**Fig. 1.** En face optical sections of a principal cell. Sectioning begins at the basal cell pole (panel *a*) and extends down to the last traceable section at the apical pole (panel *h*)

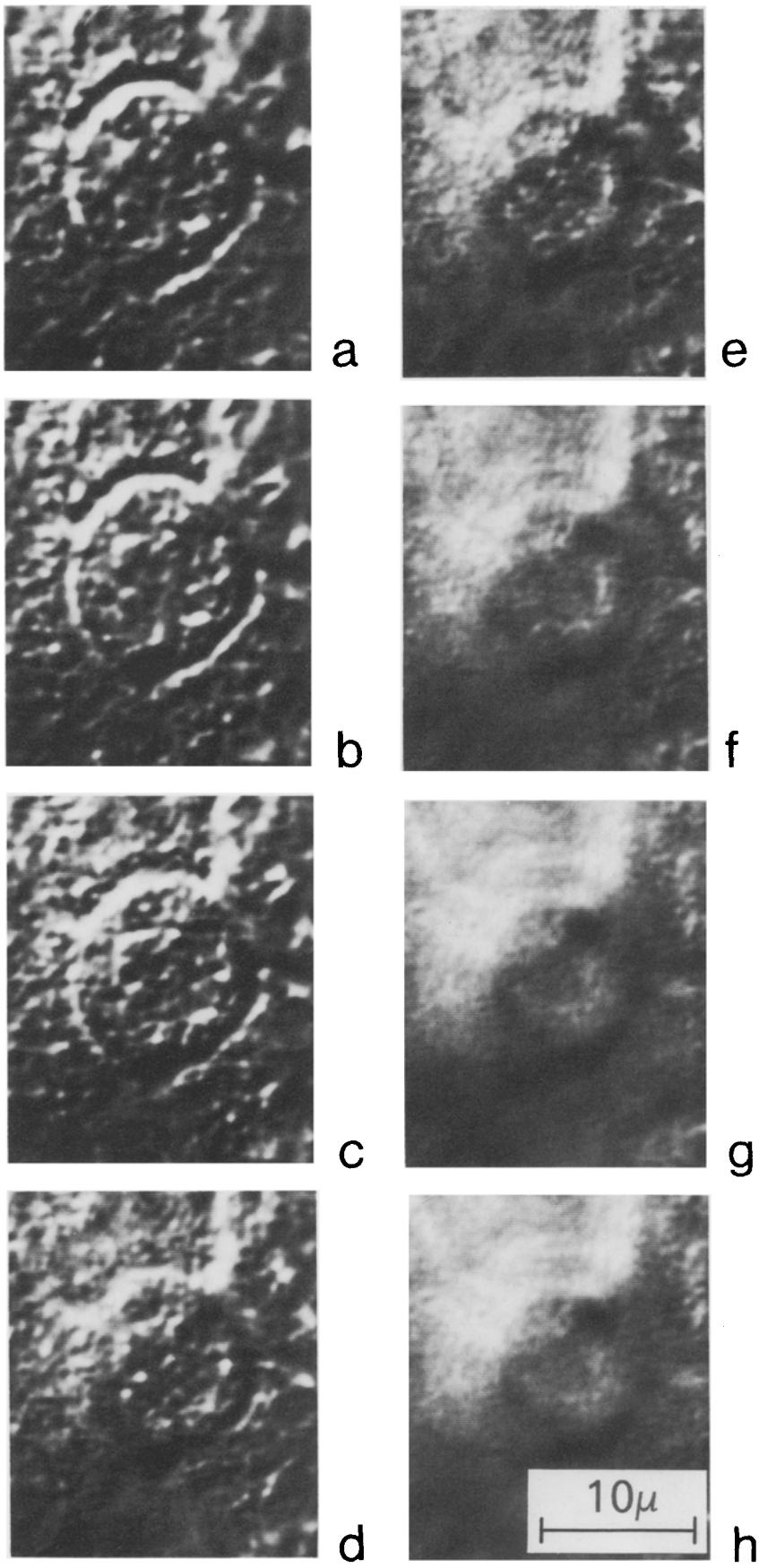


**Fig. 2.** En face optical sections of an intercalated cell. Sectioning begins at the basal pole (panel *a*) and extends down to the last traceable section at the apical pole (panel *g*)

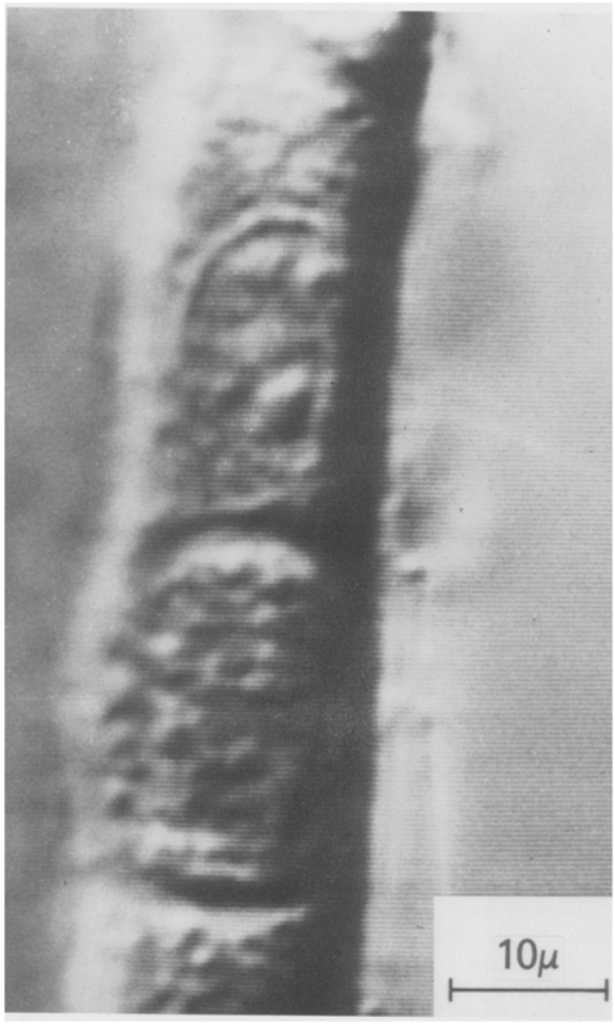


**Fig. 3.** Lateral tubule wall image of a principal (top) and an intercalated cell (bottom)

could not differentiate between the two types of intercalated cells in lateral tubule wall images.

For measurements of membrane $P_{osm}$, we chose to treat the intercalated cells as a single cell population. Intercalated cell volumes were normally distributed; there were no apparent variations in the distribution of cell membrane water permeability values or in the relative changes of cell volume and cross-sectional area induced by solution osmolality changes.

## Cell Volume Measurements

Mean cell volumes for principal and intercalated cells were 970.4 ± 30.9 $\mu m^3$ ($n$ = 45) and 643.5 ± 30.3 $\mu m^3$ ($n$ = 39), respectively (Table 1). Optical sectioning was begun at the basal pole of the cell at the first point where cellular detail was in sharp focus. Smoothed basal surface area was determined from the basal optical section with the largest cross-sectional area, typically the second or third slice (e.g., Figs. 1 and 2, Plate *c*). Smoothed lateral surface area was calculated from the perimeters of optical sections and the depth of focal displacement from the first basal section to the level of the tight junction (Table 1). We found that cell perimeter gradually decreased up to a level near the apex of each cell type and then rapidly decreased forming a domed apical pole. We arbitrarily chose the point at which the apical dome formed as the level of the tight junction. Smoothed apical surface area was determined from the cross-sectional area of the optical section at the level of the tight junction (Table 1).

Membrane surface area was corrected for infolding using the data of Wade et al. [39]. For each experiment we calculated a smoothed basolateral or apical surface area/cell volume ratio. A membrane amplification factor was then calculated by dividing the basolateral or apical surface area/cell volume ratios determined by Wade et al. [39] by our smoothed surface area/cell volume ratios. Smoothed basolateral or apical surface area was then multiplied by this amplification factor to give total membrane surface area (Table 1).[1]

## Measurement of Rates of Cell Volume Changes

Because of its slowness, the optical sectioning technique could not be used to measure rates of cell volume change. Shrinkage of principal or intercalated cells in response to a rapid 100-mosM increase of bath osmolality was complete in *ca.* 500 to 600 msec (Fig. 4). We measured the rate of change of cell volume by determining the rate of change of a random principal or intercalated cell cross-section taken through the lateral tubule wall. Implicit in this procedure was the assumption that the cell volume changed in a symmetrical manner and that the rate of change of the area of a random cross-section was

[1] It should be noted here that the principal and intercalated cell volumes determined by Wade et al. [39] are *ca.* 40 to 50% smaller than our measured cell volumes. Cell shrinkage during fixation for electron microscopy could account for some of this discrepancy. The smaller cell volumes, if due to fixation artifacts, will result in an overestimate of true membrane surface area in our studies and an underestimate of $P_{osm}$ values. However, both apical and basolateral $P_{osm}$ should be underestimated to the same degree and the ratio of the two permeabilities remain unchanged. Thus, our final conclusions regarding apparent ADH-induced cell swelling are not altered.

**Table 1.** Cell volume and membrane surface area[a]

| Cell type | Cell volume | Smooth basolateral surface area | Smooth apical surface area | Total basolateral surface area | Total apical surface area |
|---|---|---|---|---|---|
| Principal cell | 970.4 ± 30.9 $\mu m^3$ | 454.9 ± 14.8 $\mu m^2$ | 108.3 ± 5.9 $\mu m^2$ | 3,034.2 ± 98.7 $\mu m^2$ | 360.6 ± 19.7 $\mu m^2$ |
| (*n*) | (45) | (25) | (20) | | |
| Intercalated cell | 643.5 ± 30.3 $\mu m^3$ | 369.1 ± 16.1 $\mu m^2$ | 62.2 ± 3.1 $\mu m^2$ | 1,583.4 ± 69.1 $\mu m^2$ | 176.0 ± 8.8 $\mu m^2$ |
| (*n*) | (39) | (22) | (16) | | |

[a] Total basolateral and apical membrane surface area was calculated using a mean amplification factor and measured smooth basolateral and apical surface area (*see* Results).

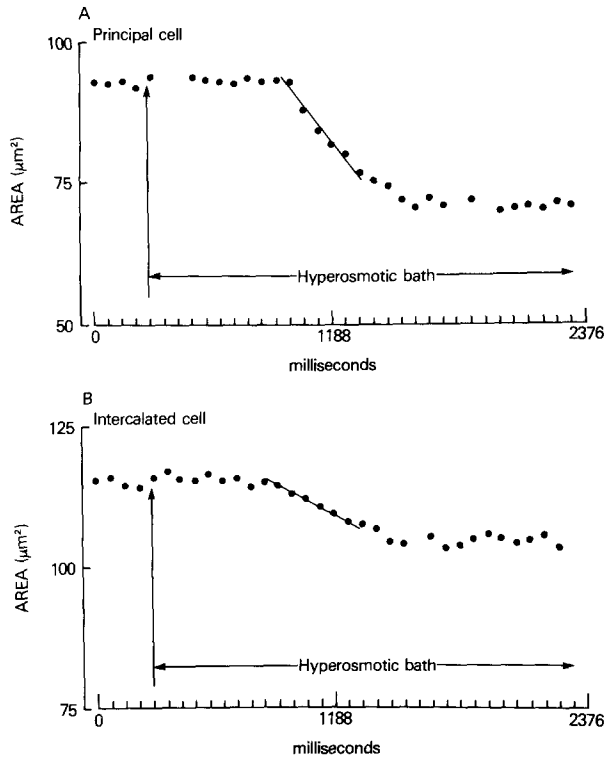


**Fig. 4.** Rates of change of the cross-sectional area of a principal and an intercalated cell in response to a rapid increase of bath osmolality from 290 to 390 mosM. The vertical arrow in each graph indicates the point at which the solenoid valves were switched. Approximately 300 msec (4 to 5 video frames) are required before the new solution reaches the bath chamber An additional 300 msec is required before measurable volume changes occur

indicative of that occurring in the entire cell. We tested this assumption by measuring cell volume before and immediately after exposure of cells to a 100-mosM hyperosmotic bathing medium and comparing the relative change in cell volume to the relative change in cell cross-sectional area. Optical sections were recorded 1 to 2 min after solution switches and before we could detect significant volume regulatory behavior by the cross-sectional area method. Data in Table 2 demonstrate that the mean percent changes in cell volume and cross-sectional area are not significantly different for either principal or intercalated cells. Since the final steady-state area and volume changes are in agreement, we conclude that the rates of volume and area change occur symmetrically.

**Table 2.** Relative changes in cell volume and cross-sectional area[a]

| Cell type | % Cross-sectional area change | % Cell volume change |
|---|---|---|
| Principal cell | −22.6 ± 1.1% | −22.8 ± 1.0% |
| (*n*) | (10) | (8) |
| Intercalated cell | −13.2 ± 0.8% | −13.3 ± 1.3% |
| (*n*) | (9) | (8) |

[a] Cortical collecting ducts were exposed to a 390-mosM bathing solution. Steady-state volume changes were measured within 1 to 2 min of the serosal solution change.

Throughout this study we used the relative change in cell cross-sectional area as a measure of relative cell volume change. Small changes (2 to 3%) in cell cross-sectional area could be accurately quantified by imaging a random cell cross-section in the lateral tubule wall. Repeated tracing of any individual cross-section typically produced a mean coefficient of variation of 1.02 ± 0.15% ($n$ = 18; data range = 40.4 − 113.6 $\mu m^2$). Conversely, we estimated that we could at best detect a minimum cell volume change of *ca.* 5 to 7% using the optical sectioning method. The mean coefficient of variation for cell volume determined by the sectioning method was 5.7 ± 0.8% ($n$ = 7; data range = 629.2 to 1346.3 $\mu m^3$).

Membrane $J_v$ and $P_{osm}$ were determined from initial rates of cell cross-sectional area changes following changes in either mucosal or serosal osmolality. When bathing solution osmolality was altered, cell volume changed exponentially until a

**Table 3.** Cell cross-sectional area changes[a]

| Cell type | Serosal osmotic gradient (mosM) | % Change cross-sectional area | Ideal % change |
|---|---|---|---|
| Principal cell | +100 | −22.6 ± 1.1% (10) | −26.4% |
| Principal cell | + 50 | −12.3 ± 2.1% (3) | −14.7% |
| Principal cell | +150 | −32.5 ± 1.2% (7) | −34.1% |
| Principal cell | −100 | 32.4 ± 2.4% (13) | 52.6% |
| Intercalated cell | +100 | −14.5 ± 0.6% (23) | −26.4% |
| Intercalated cell | + 50 | − 7.7 ± 1.6% (3) | −14.7% |
| Intercalated cell | +150 | −30.5 ± 1.9% (6) | −34.1% |
| Intercalated cell | −100 | 24.9 ± 2.4% | 52.6% |

[a] Tubules were perfused with normal (290 mosM) control solutions. Column 3 gives the area changes expected for a perfect osmometer. Steady-state area changes were measured within 1 to 2 min of the serosal solution change.

**Table 4.** Cross-sectional area changes in tubules with oil-filled lumens[a]

| Cell type | Serosal osmotic gradient (mosM) | % Change cross-sectional area |
|---|---|---|
| Principal cell | +100 −ADH | −23.4 ± 1.5% (4) |
| Principal cell | +100 +ADH | −23.2 ± 1.8% (3) |
| Intercalated cell | +100 −ADH | −16.3 ± 0.9% (4) |
| Intercalated cell | +100 +ADH | −16.1 ± 1.7% (4) |

[a] Tubules were initially perfused as described in Materials and Methods. Shortly before raising serosal osmolality to 390 mosM, tubule lumens were filled with a low-viscosity silicone oil. Predicted area change is −26.4% for a perfect osmometer (*see* Table 3). Steady-state area changes were measured within 1 to 2 min of the serosal solution change.

new steady state was reached. Rates of change were approximated from such exponential functions using linear regression analysis of the initial points. Because of measurement speed limitations, the exponential character of cell volume changes in the collecting duct was not always observable. The first 4 to 6 points of the cross-sectional area change curve showed a linear relationship ($r \geq 0.99$) and were used for rate determination. For a basolateral osmolality increase of 100 mosM, the initial linear shrinkage rate lasted *ca.* 300 msec (Fig. 4) for both principal and intercalated cell types. The cross-sectional area changes measured in each video frame for all experimental perturbations ranged between 2 and 4%.

## Osmotic Relations of Principal Cells

Data in Table 3 show the relative changes in principal and intercalated cell cross-sectional area and those changes expected for a perfect osmometer. For increases in bath osmolality, principal cells respond as osmometers with apparent water contents of 82 to 87%. These values are very similar to water contents measured in other epithelial cells [27, 28], symmetrical cells [12], and mammalian cortical kidney slices [42].

When principal cells were exposed to decreases in serosal osmolality of 100 mosM, they swelled less than predicted (Table 3). The discrepancy between this result and those obtained with hyperosmotic solutions may be partly related to tracing inaccuracies. A large degree of cell swelling causes tissue distortion and a dramatic loss of cell contrast making it difficult to accurately locate the original cell borders traced in control cells. Part of the discrepancy is also likely due to the presence of transport mechanisms moving solute and water rapidly out of the cell. As discussed below, principal cells show a significant capacity for volume regulatory decrease when exposed to hypoosmotic media.

**Table 5.** Cell volume and cross-sectional area changes in tubules bathed with silicone oil[a]

| Cell type | Mucosal osmotic gradient (mosM) | % Change cross-sectional area | % Change cell volume |
|---|---|---|---|
| Principal cell | +100 −ADH | −22.0 ± 1.2% (3) | −25.8 ± 1.4% (8) |
| Principal cell | +100 +ADH | −21.6 ± 1.3% (8) | −23.3 ± 2.5% (3) |
| Intercalated cell | +100 −ADH | −21.0 ± 1.2% (4) | −26.3 ± 1.1% (5) |
| Intercalated cell | +100 +ADH | −25.9 ± 1.4% (6) | −26.7 ± 0.3% (3) |

[a] Tubules were initially perfused as described in Materials and Methods. Shortly before raising mucosal osmolality to 390 mosM, tubules were isolated in a droplet of silicone oil. Predicted area change is −26.4% for a perfect osmometer (*see* Table 3). Steady-state area changes were measured within 1 to 2 min of the mucosal solution change.

### Osmotic Relations of Intercalated Cells

When exposed to increases in serosal osmolality of 50 and 100 mosM, intercalated cells shrank 7.7 and 14.5%, respectively. This shrinkage is less than the amount expected for an ideal osmometer (Table 3). This discrepancy is not due to water flow across the apical cell membrane. If the tubule lumen is blocked with oil to prevent water movement across that membrane, intercalated cells shrink to the same extent when bath osmolality is increased by 100 mosM (Table 4). However, when collecting ducts are bathed with silicone oil and luminal osmolality is increased by 100 mosM, intercalated cells shrink 21 to 25%. Under these conditions the ratio of observed intercalated cell area change to expected change is similar to that of principal cells (Table 5). These results, taken together with the observation that at least some intercalated cells show volume regulatory increase capabilities (*see below*), suggest the presence of a basolateral transport step moving solute and water rapidly into the cell.

Intercalated cells exposed to hypoosmotic bathing media (190 mosM) responded far less than a perfect osmometer in a manner similar to that observed in principal cells (Table 3). As with the principal cells, intercalated cells showed significant volume regulatory decrease capacity (*see below*) indicating the presence of solute and water extrusion mechanisms.

### Cell Volume Regulation

Volume regulatory decrease was clearly evident in both principal and intercalated cells. Following exposure to 190 mosM serosal medium, principal cells swelled to 133 ± 3.9% ($n$ = 6) of their control volume. The cells then shrank until they had reached a new volume within 30 min equivalent to 114.3 ± 3.2% ($n$ = 6) of control (Fig. 5). Intercalated cells swelled to 124.2 ± 3.6% ($n$ = 6) of control volume and then shrank to 105.8 ± 1.6% ($n$ = 6) of control volume after a 30-min exposure to hypoosmotic medium (Fig. 6).

We also examined volume regulatory behavior in collecting duct cells exposed to 390 mosM bathing medium. Principal cells initially shrank −24.6 ± 1.9% ($n$ = 5) and remained shrunken for at least 40 min (volume at 20 to 40 min remained below control by −25.0 ± 2.0%; $n$ = 5). Intercalated cells responded in a considerably different manner. We observed what appeared to be two physiologically distinct populations of intercalated cells (Fig. 7). One group of cells initially shrank −15.4 ± 1.1% ($n$ = 7) and remained shrunken for at least 20 to 40 min (volume remained below control at 20 to 40 min by −15.4 ± 1.1%; $n$ = 7). A second group of intercalated cells initially shrank −15.6 ± 1.1% ($n$ = 5) and after 20 to 40 min returned to within 96% of their control volume (volume at 20 to 40 min was only −4.2 ± 0.9% below that of control; $n$ = 5). These physiologically distinct intercalated cell types may be closely related to the morphological and other functional differences discussed earlier. Exposure of collecting ducts to hyperosmotic media for more than 20 to 40 min caused significant morphological changes in this epithelium. We commonly observed formation of "vacuoles," interspace distension, and cell blebbing. When these changes were observed the experiments were terminated.

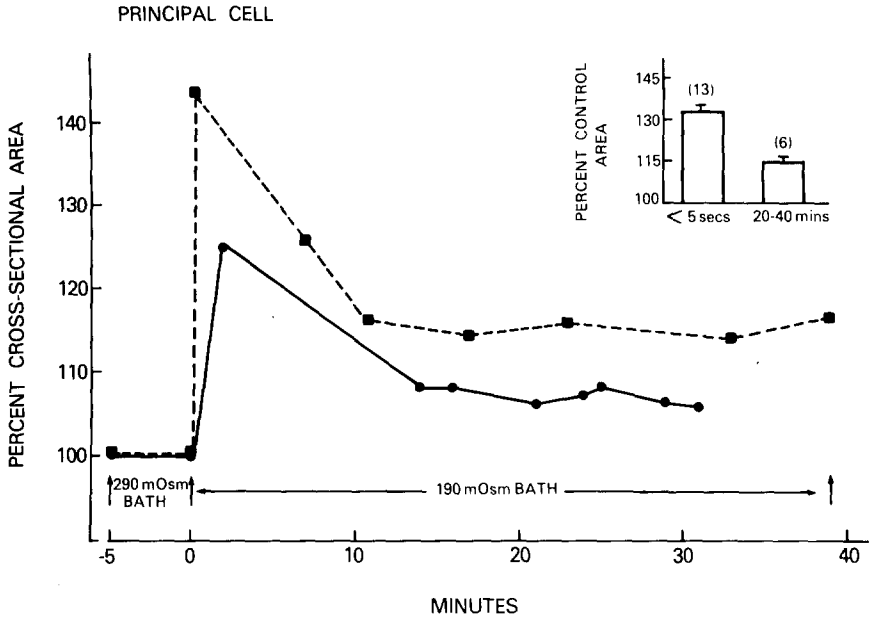


**Fig. 5.** Volume regulatory decrease in principal cells exposed to a 190-mosM basolateral bathing solution. The two tracings represent volume changes in two separate cells. Inset shows mean cell volume changes. The number of tubules is shown in parentheses above each bar

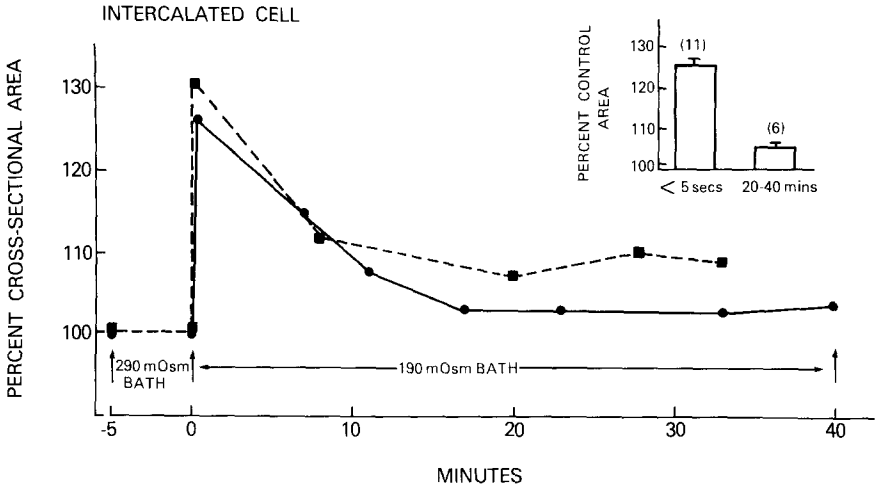


**Fig. 6.** Volume regulatory decrease in intercalated cells exposed to a 190-mosM basolateral bathing solution. The two tracings represent volume changes in two separate cells. Inset shows mean cell volume changes. The number of tubules is shown in parentheses above each bar

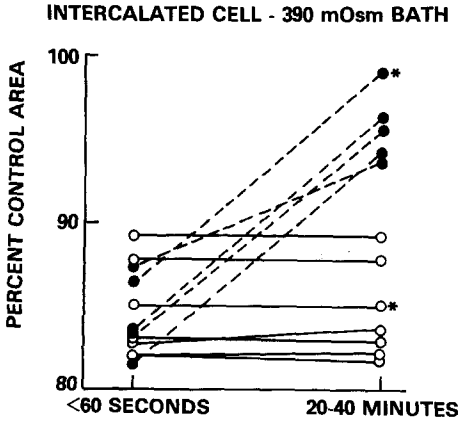


**Fig. 7.** Volume regulatory increase in intercalated cells exposed to a 390-mosM basolateral bathing solution. The asterisk denotes volume regulatory behavior in two cells from the same tubule

## Basolateral Cell Membrane Water Permeability

Cell membrane water permeability was calculated using the equation

$$J_v = L_p \sigma \Delta\Pi \quad (1)$$

where $J_v$ is the initial rate of osmotic volume flow, $L_p$ is the membrane hydraulic conductivity coefficient, $\sigma$ is the solute reflection coefficient (assumed to be 1 for raffinose), and $\Delta\Pi$ is the transmembrane osmotic gradient. Basolateral membrane $J_v$ was determined at 3 to 4 different osmolalities assuming the cell was isosmotic to the serosal bathing medium at the start of each experiment. The initial $J_v$ into or out of the cell was plotted against $\Delta\Pi$ for

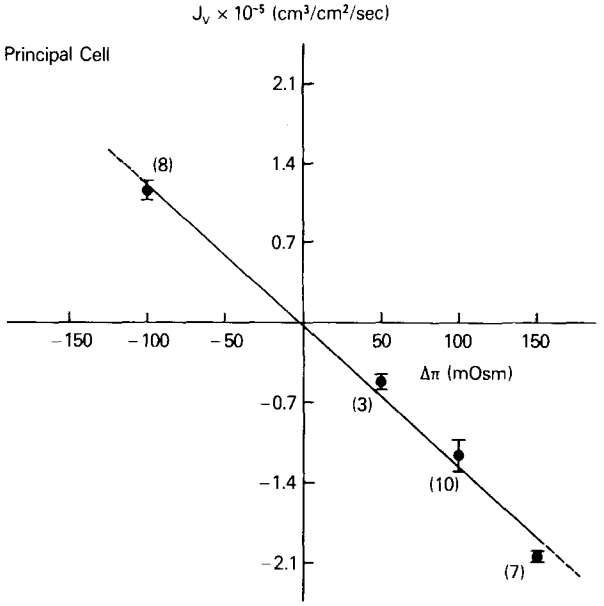


**Fig. 8.** Relationship between $J_v$ and ΔΠ for the basolateral membrane of principal cells

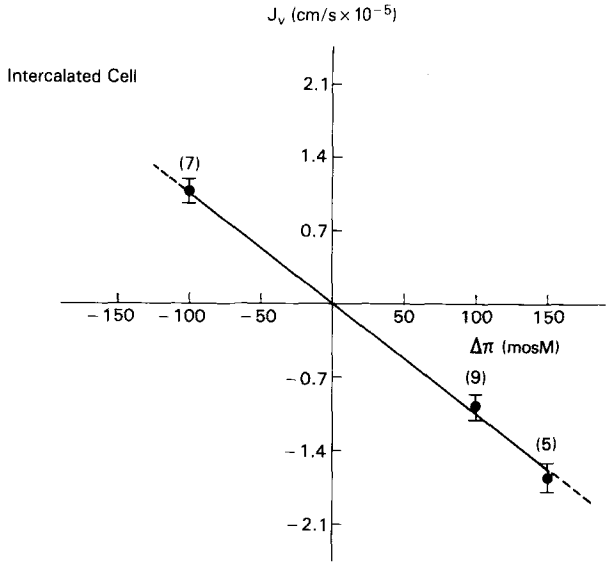


**Fig. 9.** Relationship between $J_v$ and ΔΠ for the basolateral membrane of intercalated cells

**Table 6.** Surface area-corrected basolateral membrane water permeability[a]

| Cell type | Osmotic gradient (mosM) | Osmotic $J_v$ (cm/sec × $10^{-5}$) | $P_{osm}$ ($\mu$m/sec) |
|---|---|---|---|
| Principal cell | +150 | −1.98 ± 0.02 | 73.6 ± 4.8 |
| (*n*) | | (7) | |
| Principal cell | +100 | −1.18 ± 0.13 | 66.0 ± 6.0 |
| (*n*) | | (10) | |
| Principal cell | + 50 | −0.52 ± 0.01 | 58.3 ± 10.4 |
| (*n*) | | (3) | |
| Principal cell | −100 | 1.17 ± 0.09 | 65.2 ± 4.8 |
| (*n*) | | (8) | |
| Intercalated cell | +150 | −1.85 ± 0.12 | 68.5 ± 4.8 |
| (*n*) | | (5) | |
| Intercalated cell | +100 | −1.12 ± 0.15 | 62.3 ± 8.4 |
| (*n*) | | (9) | |
| Intercalated cell | −100 | 1.02 ± 0.12 | 57.2 ± 6.7 |
| (*n*) | | (7) | |

[a] Basolateral membrane $J_v$ and $P_{osm}$ determined for principal and intercalated cells at various osmotic gradients.

both principal and intercalated cells. The relationship should be linear with an intercept of zero for a membrane with a constant apparent water permeability. Data in Figs. 8 and 9 and Table 6 demonstrate clearly that the relationship is indeed linear for both principal and intercalated cells. The smallest ΔΠ for which we could accurately measure $J_v$ in principal cells was +50 mosM. The rate of cross-sectional area change for intercalated cells was too small to measure accurately at a ΔΠ of +50 mosM. Mean *surface area-corrected* basolateral $P_{osm}$ values for principal and intercalated cells measured at a ΔΠ of +100 mosM were 66.0 ± 6.0 $\mu$m · $sec^{-1}$ ($n$ = 10) and 62.3 ± 8.4 $\mu$m · $sec^{-1}$ ($n$ = 9), respectively. These values were not statistically different ($P > 0.1$) from each other or from the $P_{osm}$ values measured at different osmolalities (*see* Table 6).

## Apical Cell Membrane Water Permeability

Measurement of apical $P_{osm}$ was greatly complicated by the extremely high basolateral water permeability. When luminal osmolality was increased

**Table 7.** Cell cross-sectional area changes-390 mosM lumen, 290 mosM bath[a]

| Cell type | −ADH | +ADH |
|---|---|---|
| Principal cell | 0 | −4.4 ± 0.5% |
| (*n*) | (6) | (7) |
| Intercalated cell | 0 | −5.5 ± 0.3% |
| (*n*) | (6) | (10) |

[a] Cross-sectional area changes for tubules perfused with 390 mosM saline and bathed with control (290 mosM) saline. Steady-state changes in area were measured within 1 to 2 min of changing mucosal solution composition.

by 100 mosM in the presence of a serosal bathing solution and ADH, principal and intercalated cells shrank at most 4 to 5% (Table 7). Such small changes in volume could not be used to accurately estimate apical $P_{osm}$. We circumvented this problem by manipulating perfused tubules into a silicone oil droplet shortly before changing the luminal solution.[2]

The silicone oil had no apparent effect on cell morphology. Indeed, the organelle movements we observed in all preparations continued unabated in tubules bathed with oil. Luminal solution switches were made within 10 min after isolating tubules in oil. This was generally the maximum working time available since droplets of condensation forming in the oil and on the coverslip beneath the oil eventually degraded image quality. Table 5 gives the measured changes in cross-sectional area, cell volume and osmotic responsiveness of both principal and intercalated cells bathed with silicone oil.

Data in Fig. 10 show rates of cross-sectional area change for a principal and intercalated cell exposed to a 390-mosM mucosal perfusate and serosal ADH. Mean *surface area-corrected* apical $P_{osm}$ values, measured in the absence of ADH at a $\Delta\pi$ of +100 mosM for principal and intercalated cells, were 19.8 ± 1.9 $\mu m \cdot sec^{-1}$ ($n$ = 10) and 25.0 ± 2.3

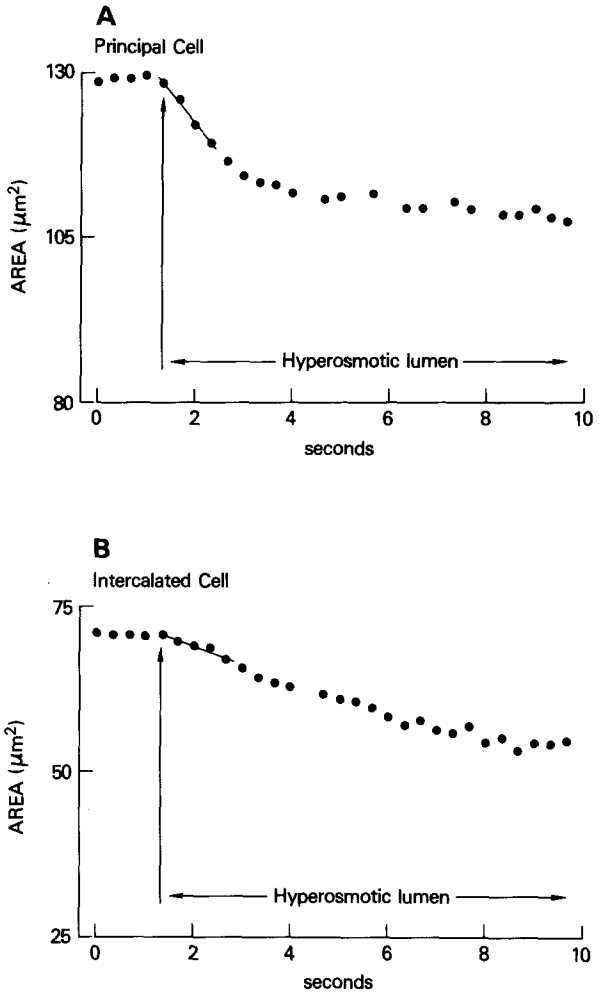


**Fig. 10.** Rates of change of the cross-sectional area of a principal and intercalated cell in response to a rapid increase of luminal osmolality from 290 to 390 mosM. Cells were exposed to a supramaximal dose of ADH for 30 min before tubules were isolated in a small droplet of silicone oil. The vertical arrow in each graph indicates the point at which the luminal perfusates were changed

$\mu m \cdot sec^{-1}$ ($n$ = 8), respectively (Table 8). Vasopressin increased apical $P_{osm}$ in principal cells about four- to fivefold to 92.2 ± 8.6 $\mu m \cdot sec^{-1}$ ($n$ = 10). In addition, ADH appeared to increase apical $P_{osm}$ of intercalated cells to 86.2 ± 6.0 $\mu m \cdot sec^{-1}$ ($n$ = 8).

We also tested the effect of ADH on basolateral $P_{osm}$. Shortly before increasing bath osmolality to 390 mosM, control or ADH-treated tubules were filled with Dow-Corning 200 silicone oil (1 cs viscosity) to prevent apical water flow. Oil was injected using a double-barrel pipette arrangement [15] or an exchange pipette system [5]. Table 9 indicates that ADH has no statistically significant ($P > 0.2$) effect on principal or intercalated cell basolateral $P_{osm}$. In addition, these data demonstrate that, in the absence of ADH, basolateral $P_{osm}$ measurements in tubules

[2] Perfusion of isolated renal tubules under oil has been used with a high success rate to collect absorbates and study water reabsorption in proximal nephrons [2]. The success rate in cortical collecting ducts, however, was extremely low. Approximately 80% of all tubules isolated in the oil collapsed completely and it was impossible to reopen the lumen with increases in perfusion pressure. Tubule collapse presumably occurred because of the high interfacial tension within the oil droplet. The different behavior of cortical collecting ducts and proximal tubules under oil may be due to a difference in basement membrane stiffness in the two segments. In an attempt to alleviate this problem we tested a number of different oils and fluorocarbons but were unable to improve our success rate. Ultimately we used silicone oil for our experiments because paraffin oils rotated the plane of polarized light and degraded image quality.

**Table 8.** Surface area-corrected apical membrane water permeability[a]

| Cell type | Osmotic $J_v$ (cm/sec × $10^{-5}$) | $P_{osm}$ ($\mu$m/sec) |
|---|---|---|
| Principal cell (*n*) | −0.36 ± 0.04 (10) −ADH | 19.8 ± 1.9 |
| Principal cell (*n*) | −1.83 ± 0.23 (10) +ADH | 92.2 ± 8.6 |
| Intercalated cell (*n*) | −0.45 ± 0.04 (8) −ADH | 25.0 ± 2.3 |
| Intercalated cell (*n*) | −1.55 ± 0.11 (8) +ADH | 86.2 ± 6.0 |

[a] Apical membrane osmotic $J_v$ and $P_{osm}$ of principal and intercalated cells. Values were determined at a single osmotic gradient of +100 mosM.

**Table 9.** Surface area-corrected basolateral membrane water permeability in tubules with oil-filled lumens[a]

| Cell type | Osmotic $J_v$ (cm/sec × $10^{-5}$) | $P_{osm}$ ($\mu$m/sec) |
|---|---|---|
| Principal cell (*n*) | −1.23 ± 0.06(4) −ADH | 68.2 ± 3.5 |
| Principal cell (*n*) | −1.33 ± 0.10(3) +ADH | 74.1 ± 5.8 |
| Intercalated cell (*n*) | −1.27 ± 0.08(4) −ADH | 70.5 ± 4.6 |
| Intercalated cell (*n*) | −1.10 ± 0.17(3) +ADH | 61.2 ± 9.6 |

[a] Basolateral membrane $J_v$ and $P_{osm}$ values determined at an osmotic gradient of +100 mosM in the presence and absence of ADH. Tubule lumens were filled with oil shortly before the basolateral solution switch.

perfused with saline are not affected by apical water movement. Basolateral $P_{osm}$ values for principal and intercalated cells were not statistically different ($P > 0.4$) in tubules perfused with saline or oil (*cf.* Tables 6 and 9).

## Discussion

This work is the first direct determination of the water permeabilities of the cell membranes of mammalian cortical collecting duct. The technical complexity and methodological difficulties of these measurements constitute significant potential sources of error. Therefore, we first discuss the methodological considerations and then the physiological implications of the results.

### Methodology

To obtain accurate measurements of plasma membrane $P_{osm}$ in an epithelial or symmetrical cell, it is necessary to rigorously fulfill three important experimental requirements: (1) rapid step changes in extracellular osmolality, (2) absence of significant external unstirred layers adjacent to the preparation or knowledge of the size of these layers, (3) measurement of initial or peak osmotically induced volume flow rates across the cell membrane.

Our laminar flow bath chamber permitted rapid ($t_{1/2}$ = 55 msec) changes in serosal bathing solution composition without significant disturbance of tubule focus or position. The minimum $t_{1/2}$ for cell volume changes induced by serosal osmolality gradients was *ca.* 300 msec. A retractable pipette system allowed for fast ($t_{1/2}$ = 70 to 150 msec) luminal solution switches without tubule movement. Cell volume changes induced by luminal osmolality increases in the presence of serosal ADH had a $t_{1/2}$ of *ca.* 1.5 sec. The retractable pipette method is particularly well-suited for apical $P_{osm}$ measurements in isolated tubules. The solution changes constitute step changes in osmolality for all practical purposes and correction for the time course of the osmolality change was not needed.

The presence of large unstirred layers adjacent to cell membranes causes significant underestimates of $P_{osm}$ [3]. We measured serosal unstirred layer thickness in the regions where volume measurements were made by observing the flow pattern of latex beads around the tubule [35]. Unstirred layers generated by vortex formation and turbulent flow at the tubule-solution interface are ≤ 3 $\mu$m thick and should have a negligible effect on our $P_{osm}$ measurement. Because of the small tubule radius, luminal unstirred layers are expected to be insignificant and should have a minimal effect on $P_{osm}$ measurements at the apical membrane.

At this time, we do not know how to evaluate the effects of putative cytoplasmic and interspace unstirred layers on our $P_{osm}$ measurements. The linear relationship between $J_v$ and $\Delta\Pi$ for the basolateral membranes of principal and intercalated cells (Figs. 8 and 9) suggest that they do not cause a significant underestimate of $P_{osm}$. Water flow across the basolateral membrane is much higher than that across the apical membrane and therefore basolateral $P_{osm}$ should be underestimated to a greater degree than apical $P_{osm}$ by intraepithelial unstirred layers. Thus, the ratio of basolateral to apical $P_{osm}$ should be even higher than the value we have calculated.

Cell volume changes induced by osmotic gradients alter cell osmolality and therefore the transmembrane driving force for fluid movement. Conse-

quently, it is necessary to measure initial or peak $J_v$ for accurate determination of membrane $P_{osm}$. In this study, $J_v$ was determined from the initial rate of cell cross-sectional area change. Our results support the assumption that cell volume changes symmetrically, and that the rate of change of cross-sectional area could be used as a measure of the rate of cell volume change. This approach allowed measurement of very small (*ca.* 2%) changes in cell volume with a minimum time of resolution of 66 msec. Transmembrane volume flow was approximately constant in these experiments for the first 4 to 6 time points of the area change curve and then slowed as cell osmolality was significantly altered. Fitting an exponential to the time course of the cell area change did not significantly alter the value of $J_v$ determined.

### Basolateral Membrane $P_{osm}$

Equation (1) can be used to calculate $L_p$ or $P_{osm}$ only if the relationship between $J_v$ and $\Delta\pi$ is linear and therefore the membrane has a constant apparent water permeability. Deviations from a linear relationship can be caused by a number of factors including intracellular and extracellular unstirred layers and transport mechanisms moving solute and water into or out of the cell at rates similar to the rate of osmotically induced volume flow. Our results demonstrate that the relationship between basolateral $J_v$ and $\Delta\pi$ is linear for both principal and intercalated cells. These data further validate our methodological approach and demonstrate that the basolateral membrane of both cell types has a constant $P_{osm}$ over a wide range of osmolalities. Furthermore, these results demonstrate the absence of rectification of water flow across the basolateral membrane. Water flow rectification has been reported in a wide variety of cells and tissues [21], but has only been extensively studied in the human red blood cell. In this cell type, recent studies have demonstrated that the apparent rectification is an artifact of the cell volume measuring technique [37].

The mean *surface area-corrected* basolateral $P_{osm}$ value for principal and intercalated cells were 66 and 62 $\mu m \cdot sec^{-1}$, respectively. These values are remarkably similar to area-corrected permeabilities determined for *Necturus* gallbladder apical (68 $\mu m \cdot sec^{-1}$) and basolateral (46 $\mu m \cdot sec^{-1}$) cell membranes [33] and are comparable to osmotic permeabilities determined in a number of other cell types (for reviews, *see* refs. 4, 19). Such permeabilities are within the wide range of $P_{osm}$ values determined for a variety of artificial lipid membranes where water traverses the bilayer via solubility-diffusion processes (e.g., refs. 10, 11).

Basolateral $P_{osm}$ was also measured in the presence of ADH. Recent studies [9, 20, 21] have suggested that ADH may increase the permeability of a barrier distal to the apical membrane in toad bladder epithelial cells. Kachadorian et al. [21] suggested that this barrier may be the basolateral cell membrane. Since the toad bladder is commonly used as a model for understanding mammalian distal nephron function, we tested this hypothesis directly in the cortical collecting duct. Our results demonstrate that ADH has no significant effect on basolateral $P_{osm}$ in collecting duct.

### Principal Cell Apical Membrane $P_{osm}$

Because of the very high basolateral membrane water permeability, it was necessary to measure $P_{osm}$ in tubules bathed with silicone oil. In the absence of ADH, *surface area-corrected* apical membrane $P_{osm}$ for principal cells was 20 $\mu m \cdot sec^{-1}$. Taking into account differences in membrane surface areas [39], the entire basolateral membrane of a principal cell is about 27 times more water permeable than the entire apical membrane. Osmotic permeability of the apical membrane increases four- to fivefold to 92 $\mu m \cdot sec^{-1}$ in the presence of serosal ADH. Under these conditions, the total basolateral water permeability of a principal cell was still six- to sevenfold greater than apical membrane permeability. From these permeability values, one can predict that principal cells should shrink only 5 to 6% when mucosal osmolality is increased by 100 mosM and a normal serosal bath and ADH are present. The actual cell volume shrinkage measured was 4 to 5% (Table 7). Such results provide strong support for the quantitative accuracy of our $P_{osm}$ measurements.

The conclusion that the $P_{osm}$ of the basolateral membrane is always much greater than that of the apical membrane disagrees with previous studies [13, 24]. On the basis of the magnitude of the apparent cell swelling induced by exposure of the tissues to luminal hypotonicity in the presence of supramaximal ADH, these investigators concluded that the apical and basolateral $P_{osm}$ were approximately equal. These indirect estimates of the relative $P_{osm}$ of the cell membranes have been recently shown to be incorrect because of misinterpretation of the changes in epithelial geometry induced by the hypotonic perfusates [36].

### Intercalated Cell Apical Membrane $P_{osm}$

In the absence of ADH, we measured a *surface area-corrected* apical $P_{osm}$ for intercalated cells of 25 $\mu m \cdot sec^{-1}$. Apical $P_{osm}$ increased four- to five-

fold with serosal ADH addition to a value of 86 $\mu m \cdot sec^{-1}$. The ratios of entire basolateral cell membrane osmotic permeability/entire apical cell membrane osmotic permeability for the intercalated cell in the absence or presence of ADH were 17 and 5, respectively.

These results appear to indicate that the intercalated cells respond to ADH with an increase in apical water permeability. However, another possibility is that the water movements into or out of intercalated cells occur primarily across the basolateral membrane. Because of the relatively small interspace volume/cell volume ratio and the presence of oil in the serosal bath, it would be expected that interspace osmolality would be largely determined by principal cell osmolality. Thus, as principal cells shrink, interspace osmolality would increase rapidly causing water flow across the highly permeable basolateral membrane of intercalated cells. Inasmuch as measurements of apical $P_{osm}$ required oil in the serosal bath, there was no way to experimentally determine apical $P_{osm}$ uninfluenced by this potential artifact. Instead, we utilized a compartmental model to estimate the maximum interspace osmolality changes which would be produced by principal cell shrinkage when a normal, flowing serosal bath was present. The model was developed and the calculations done by Dr. C. Patlak (NIH). The interspace was modeled as a rectangular slit with no lateral or longitudinal tortuosity [40] and a width of 0.5 $\mu m$ (K. Strange, *unpublished observation*). Solutes and water were assumed to diffuse freely within the interspace. We also assumed that principal cell osmolality increased to 390 mosM when luminal osmolality was raised to 390 mosM. Based on the small volume changes (−4.4%; *see* Table 7) observed in principal cells under these conditions, we calculate that cell osmolality would actually increase to 305 mosM rather than the 390 mosM utilized in the model calculation. Using this "worst" case assumption, we calculated that interspace osmolality could be increased to only 293 mosM. Furthermore, this osmolality increase would be localized to the apical portion of the interspace and decrease rapidly to that of the serosal solution at the basal end of the channel. Even if we assume that this interspace osmolality increase was distributed over the *entire* basolateral surface of the intercalated cells, we could expect at most a 1% shrinkage of this cell type. The actual measured intercalated cell volume changes when luminal osmolality was raised to 390 mosM in the presence of serosal ADH was −5.5% (Table 7). This value is remarkably close to the expected shrinkage of 6 to 7% predicted from measured $P_{osm}$ values and relative membrane surface areas [39]. Thus, the model calculations support the hypothesis that intercalated cells respond to ADH with an increase in apical $P_{osm}$.[3]

Previous studies in toad bladder have shown the presence of an ADH-sensitive adenylate cyclase [16, 32] in isolated toad bladder mitochondria-rich cells. These observations, in conjunction with our results, support the contention that ADH increases the water permeability of the intercalated cell and that these cells are involved in transepithelial water reabsorption and water homeostasis. Morphological studies conducted by others [8, 13, 24] to examine the effects of ADH on intercalated cells do not permit conclusions about the role of this cell type in water reabsorption.

Because of the technical difficulties associated with these experiments, we did not examine the relationship between apical $J_v$ and $\Delta\pi$. Transepithelial $J_v$, however, has been shown to be linearly related to $\Delta\pi$ over a wide range of osmolality gradients (−180 to 255 mosM; ref. 29). Since our results demonstrate directly that the apical membrane is the rate-limiting step for water movement across both principal and intercalated cells (*see below*), it is likely that the transepithelial $J_v$ *vs.* $\Delta\pi$ relationship reflects the characteristics of water flow across the apical membrane.

## Relationship Between Cell Membrane and Transepithelial $P_{osm}$

Transepithelial $P_{osm}$ values reported in the literature have been calculated from measured tubule length and inner diameter assuming a smooth apical surface area. Table 10 gives mean values of apical membrane $P_{osm}$ based on measured smooth apical membrane area. Apical $P_{osm}$ calculated in such a manner for the principal cell was 66 $\mu m \cdot sec^{-1}$ in the absence of ADH and 307 $\mu m \cdot sec^{-1}$ with ADH present. Our results support the previous conclusion that the apical cell membrane constitutes the primary barrier to transepithelial water movement. An estimate of transepithelial $P_{osm}$ can be made from our cell membrane $P_{osm}$ values, the relative surface areas of the membranes, and the known ra-

[3] An alternative way of viewing the problem is to compare the relative volume changes in principal and intercalated cells induced by raising luminal osmolality to 390 mosM. Even though the difference in the relative change for the two cell types is small, it is nevertheless statistically significant ($0.025 < P < 0.05$). Thus, in order for interspace osmolality to explain intercalated cell shrinkage, principal cell shrinkage would have to raise the osmolality of the fluid bathing the *entire* basolateral membrane of intercalated cells by 5.5%. Since principal cells only shrink 4.4% on average, it seems far more likely that intercalated cell shrinkage is due to water flow across an apical membrane made more water permeable by ADH.

**Table 10.** Cell membrane water permeability calculated from smooth membrane surface areas[a]

| Cell type | ADH | Apical $J_v$ (cm/sec × $10^{-5}$) | Apical $P_{osm}$ ($\mu$m/sec) |
|---|---|---|---|
| Principal cell | — | −1.18 ± 0.12 | 65.9 ± 6.4 |
| (*n*) | | (10) | |
| Principal cell | + | −5.52 ± 0.51 | 306.9 ± 28.6 |
| (*n*) | | (10) | |
| Intercalated cell | − | −1.27 ± 0.12 | 70.8 ± 6.5 |
| (*n*) | | (8) | |
| Intercalated cell | + | −4.38 ± 0.31 | 243.8 ± 17.1 |
| (*n*) | | (8) | |

[a] Cell membrane osmotic $J_v$ and $P_{osm}$ for principal and intercalated cells determined at a single osmotic gradient of +100 mosM. Values were calculated using measured smooth apical surface area without correction for membrane infolding.

tio of principal to intercalated cells. In the absence of ADH, transepithelial $P_{osm}$ is calculated to be 64.7 $\mu m \cdot sec^{-1}$, and in the presence of the hormone $P_{osm}$ rises to 241.3 $\mu m \cdot sec^{-1}$. These calculated values are in excellent agreement with transepithelial $P_{osm}$ measurements conducted at 37°C. For example, Al-Zahid et al. [1] found that transepithelial $P_{osm}$ in rabbit cortical collecting tubule in the absence and presence of ADH was 66.2 and 311.5 $\mu m \cdot sec^{-1}$, respectively.

### Cell Volume Regulation

Both principal and intercalated cells are capable of significant volume regulatory decrease after being swollen by exposure to a 190-mosM serosal bath. Principal and intercalated cells returned to within 15 and 5 to 10%, respectively, of their control volume after exposure to dilute media for 10 to 15 min. Although Kirk et al. [23] were unable to differentiate principal and intercalated cells in studies on isolated rabbit cortical collecting ducts, they observed no volume regulatory decrease behavior of whole tubules based on measurements of wall thickness. The reason for this discrepancy is most likely related to bath temperature. The studies by Kirk et al. were carried out at 25°C while our studies were conducted at 37°C. Dellasega and Grantham [7] have also observed volume regulatory decrease in nonperfused cortical collecting tubules exposed to dilute media at 37°C.

In addition to volume-regulatory decrease behavior, we examined the ability of cortical collecting ducts to increase their volume after being shrunken by exposure to 390 mosM serosal media. Principal cells show no volume-regulatory increase behavior after exposure to hypertonic media for 20 to 40 min. Intercalated cells, however, responded in a considerably different manner. There appeared to be at least two physiologically distinct groups of intercalated cells based on their volume-regulatory behavior. One group of cells showed no capacity for volume-regulatory increase whereas a second group of intercalated cells returned to within 4% of their control volume after a 20- to 40-min exposure to a 390-mosM serosal solution. Cells in the renal cortex are not normally exposed to hypertonicity of this magnitude. Prolonged exposure of cortical collecting tubules to hypertonic media causes irreversible damage to the epithelium suggesting that the cells are not physiologically adapted to hyperosmotic conditions. Volume-regulatory increase behavior most likely represents a difference in solute entry and exit steps between the different cortical collecting duct cell types.

## Conclusions

Our methodological advances have permitted the accurate determination of the cell membrane water permeability of cells of the rabbit cortical collecting duct. Our results show, in agreement with the conclusions of previous investigators utilizing indirect measurement techniques, that the apical membrane is rate limiting for transepithelial water movement in both the absence and presence of ADH. Our observations also indicate that the total basolateral membrane water permeability is at least 5 to 7 times greater than apical water permeability in collecting ducts exposed to vasopressin. Finally, we have presented data which indicate that both principal and intercalated cells are responsive to ADH, that both cell types exhibit volume regulatory decrease behavior, and that there appear to be two physiologically distinct populations of intercalated cells.

The authors wish to thank Drs. C. Patlak and D. Marsh for extensive help with computer modeling and mathematical analyses, and Dr. R. Bowman, Dr. R. Lutz and Mr. R. Paul for invaluable technical advice. We also thank J. Sullivan, C. Gibson and W. Dehn for constructing and helping to design much of the equipment used in this study, and Drs. M. Burg, J. Handler and W. Harris for critical reading of the manuscript. K. Strange was supported by a National Kidney Foundation postdoctoral fellowship.

## References

1. Al-Zahid, G., Schafer, J.A., Troutman, S.L., Andreoli, T.E. 1977. Effect of antidiuretic hormone on water and solute permeation, and the activation energies for these processes, in mammalian cortical collecting tubules: Evidence for parallel diffusion in luminal plasma membranes. *J. Membrane Biol.* **31**:103–129

2. Barfuss, D.W., Schafer, J.A. 1981. Collection and analysis of absorbate from proximal straight tubules. *Am. J. Physiol.* **241:**F597–F604
3. Barry, P.H., Diamond, J.M. 1984. Effects of unstirred layers on membrane phenomena. *Physiol. Rev.* **64:**763–872
4. Berry, C.A., 1983. Water permeability and pathways in the proximal tubule. *Am. J. Physiol.* **245:**F279–F294
5. Burg, M.B. 1972. Perfusion of isolated renal tubules. *Yale J. Biol. Med.* **45:**321–326
6. Carpi-Medina, P., Lindmann, B., Gonzales, E., Whittembury, G. 1984. The continuous measurement of tubular volume changes in response to step changes in contraluminal osmolality. *Pfluegers Arch.* **400:**343–348
7. Dellasega, M., Grantham, J. 1973. Regulation of renal tubule cell volume in hypotonic media. *Am. J. Physiol.* **224:**1288–1294
8. DiBona, D.R., Civan, M.M., Leaf, A. 1969. The cellular specificity of the effect of vasopressin on toad urinary bladder. *J. Membrane Biol.* **1:**79–91
9. Dratwa, M., Tisher, C.C., Sommer, J.R., Croker, B.P. 1979. Intramembranous particle aggregation in toad urinary bladder after vasopressin stimulation. *Lab. Invest.* **40:**46–54
10. Fettiplace, R., Haydon, D.A. 1980. Water permeability of lipid membranes. *Physiol. Rev.* **60:**510–550
11. Finkelstein, A. 1984. Water movement through membrane channels. *Curr. Top. Membr. Transp.* **21:**295–308
12. Freel, R.W. 1978. Patterns of water and solute regulation in the muscle fibres of osmoconforming marine decapod crustaceans. *J. Exp. Biol.* **72:**107–126
13. Ganote, C.E., Grantham, J.J., Mores, H.L., Burg, M.B., Orloff, J. 1968. Ultrastructural studies of vasopressin effect on isolated perfused renal collecting tubules of the rabbit. *J. Cell Biol.* **36:**355–367
14. Gonzales, E., Carpi-Medina, P., Linares, H., Whittembury, G. 1984. Osmotic water permeability of the apical membrane of proximal straight tubular (PST) cells. *Pfluegers Arch.* **402:**337–339
15. Greger, R., Schlatter, E. 1983. Properties of the lumen membrane of the cortical thick ascending limb of Henle's loop of rabbit kidney. *Pfluegers Arch.* **396:**315–324
16. Handler, J.S., Preston, A.S. 1976. Study of enzymes regulating vasopressin-stimulated cyclic AMP metabolism in separated mitochondria-rich and granular epithelial cells of toad urinary bladder. *J. Membrane Biol.* **22:**43–50
17. Hays, R.M. 1983. Alteration of luminal membrane structure by antidiuretic hormone. *Am. J. Physiol.* **245:**C298–C296
18. Hebert, S.C., Schafer, J.A., Andreoli, T.E. 1981. The effects of antidiuretic hormone (ADH) on solute and water transport in the mammalian nephron. *J. Membrane Biol.* **58:**1–19
19. House, C.R. 1974. Water Transport in Cells and Tissues. Edward Arnold, London
20. Kachadorian, W.A., Casey, C., DiScala, V.A. 1978. Time course of ADH-induced intramembranous particle aggregation in toad urinary bladder. *Am. J. Physiol.* **234:**F461–F465
21. Kachadorian, W.A., Sariban-Sohraby, S., Spring, K.R. 1985. Regulation of water permeability in toad urinary bladder at two barriers. *Am. J. Physiol.* **248:**F260–F265
22. Kaissling, B., Kriz, W. 1979. Structural analysis of the rabbit kidney. *In:* Advances in Anatomy and Cell Biology. A. Brodal et al., editors. Vol. 56, pp. 1–123. Springer, New York
23. Kirk, K. L., DiBona, D.R., Schafer, J.A. 1984. Morphologic response of the rabbit cortical collecting tubule to peritubular hypotonicity: Quantitative examination with differential interference contrast microscopy. *J. Membrane Biol.* **79:**53–64
24. Kirk, K.L., Schafer, J.A., DiBona, D.R. 1984. Quantitative analysis of the structural events associated with antidiuretic hormone-induced volume reabsorption in the rabbit cortical collecting tubule. *J. Membrane Biol.* **79:**65–74
25. Kriz, W., Kaissling, B. 1985. Structural organization of the mammalian kidney. *In:* The Kidney: Physiology and Pathophysiology D.W. Seldin and G. Giebisch, editors. Vol. 1, pp. 265–306. Raven, New York
26. Larson, M., Spring, K.R. 1984. Volume regulation by *Necturus* gallbladder: Basolateral KCl exit. *J. Membrane Biol.* **81:**219–232
27. Lau, Y.T., Parsons, R.H., Feeney, G.A., Walker, K.L. 1981. Bath osmolality: Effect on water permeability of epithelial tissue. *Am. J. Physiol.* **242:**C184–C191
28. Persson, B.E., Spring, K.R. 1982. Gallbladder epithelial cell hydraulic water permeability and volume regulation. *J. Gen. Physiol.* **79:**481–505
29. Schafer, J.A., Patlak, C.S., Andreoli, T.E. 1974. Osmosis in cortical collecting tubules. A theoretical and experimental analysis of the osmotic transient phenomenon. *J. Gen. Physiol.* **64:**201–227
30. Schwartz, G.J., Al-Awqati, Q. 1985. Two functionally distinct types of mitochondria-rich (MR) cells of cortical collecting tubules (CCT) as determined by changes in pH ($pH_i$) in individually identified cells. *Kidney Int.* **27:**288
31. Schwartz, G.J., Al-Awqati, Q. 1985. Polarity of $H^+$ transport in the two types of mitochondria-rich (MR) cells of cortical collecting tubules (CCT). *Clin. Res.* **33:**497A
32. Scott, W.N., Sapirstein, V.S., Yoder, M.J. 1974. Partition of tissue functions in epithelia: Localization of enzymes in "mitochondria-rich" cells of toad urinary bladder. *Science* **184:**797–799
33. Spring, K.R. 1983. Fluid transport by gallbladder epithelium. *J. Exp. Biol.* **106:**181–194
34. Spring, K.R., Hope, A. 1979. Fluid transport and the dimensions of cells and interspaces of living *Necturus* gallbladder. *J. Gen. Physiol.* **73:**287–305
35. Strange, K., Spring, K.R. 1986. Methods for imaging renal tubule cells. *Kidney Int.* **30:**192–200
36. Strange, K., Spring, K.R. 1987. Absence of significant cytoplasmic dilution during ADH-stimulated water reabsorption in a tight epithelium. *Science (in press)*
37. Terwilliger, T., Solomon, A.K. 1981. The osmotic water permeability of human red cells. *J. Gen. Physiol.* **77:**549–570
38. Verlander, J.W., Madsen, K.M., Tisher, C.C. 1985. Two populations of intercalated cells exist in the cortical collecting duct of the rat. *Clin. Res.* **33:**501a
39. Wade, J.B., O'Neil, R.G., Pryor, J.L., Boulpaep, E.L. 1979. Modulation of cell membrane area in renal collecting tubules by corticosteroid hormones. *J. Cell Biol.* **81:**439–445
40. Welling, L.W., Evan, A.P., Welling, D.J. 1981. Shape of cells and extracellular channels in rabbit cortical collecting ducts. *Kidney Int.* **20:**211–222
41. Welling, L.W., Welling, D.J., Ochs, T.J. 1983. Video measurement of basolateral membrane hydraulic conductivity in the proximal tubule. *Am. J. Physiol.* **245:**F123–F129
42. Whittembury, G., Grantham, J.J. 1976. Cellular aspects of renal sodium transport and cell volume regulation. *Kidney Int.* **9:**103–120

Received 13 June 1986; revised 24 November 1986